SAND2007-4444C

SHOCK CONSOLIDATION OF NANOCRYSTALLINE ALUMINUM FOR BULK COMPONENT FORMATION

D. A. Fredenburg[1,2], T. J. Vogler[2], C. J. Saldana[3], and N. N. Thadhani[1]

[1]*Material Science & Engineering, Georgia Institute of Technology, 771 Ferst Dr. Atlanta GA 30332*
[2]*Sandia National Laboratories, PO Box 5800 MS-1181, Albuquerque NM 87185*
[3]*School of Industrial Engineering, Purdue University, West Lafayette IN 47907*

Abstract. Al 6061-T6 powder particles with a partially nanocrystalline graded microstructure in three distinct morphologies are compacted at an impact velocity of 650 m/s. Recovered samples are characterized to determine degree of compaction, deformation characteristics, and mechanical properties. Compacts range from 96-98% of theoretical density, exhibiting relatively low elastic moduli. Nano-indentation yields relatively consistent hardness values of ~1.4 GPa, indicating hardness of starting powders is preserved after compaction. Micro-indentation indicates varying degrees of compaction through specimen cross-section, which is supported by EBSD and optical microscopy.

Keywords: dynamic consolidation, nanocrystalline, Al 6061-T6, mechanical properties.
PACS: 62.25.+g, 62.50.+p, 81.20.Ev.

INTRODUCTION

Partially nanocrystalline materials are of interest because they have potential to exhibit both high strength and moderate ductilities. In this study, partially nanocrystalline Al 6061-T6 particles with a graded microstructure in three morphologies are consolidated through passage of a large amplitude stress pulse. Dynamic consolidation is used because of the relatively short time durations to which particles are exposed to elevated temperatures, which is desirable for grain structure preservation. Powders acquire graded microstructures through severe plastic deformation machining.

EXPERIMENTAL PROCEDURE

All three morphology Al 6061-T6 particles used in this study were formed through severe plastic deformation machining [1]. The three morphologies, termed equiaxed, needles, and platelets, have the average dimensions given in Table 1.

Table 1. Average dimensions of aluminum particles.

Shape	Aspect Ratio	Size (µm)
Equiaxed	1 x 1 x 0.8	50 x 50 x 30
Needles	3 x 10 x 2	30 x 100 x 20
Platelets	5 x 5 x 1	80 x 80 x 30

Quasi-static pressure-density curves for each of the powders were generated for loads up to 5000 N. The data was fit using the Fischmeister-Artz relationship in the following form [2]

$$P_y = 2.97\rho^2 \left(\frac{\rho-\rho_0}{1-\rho_0}\right)\sigma_y \qquad (1)$$

assuming a constant yield strength, allowing for an estimate of powder crush strength (stress required to achieve full density). For the experiments reported here, all powders were quasi-statically pressed, uni-axially, to a starting density of 1.86 g/cm^3 inside a steel recovery capsule. A cut-away view showing one portion of the three capsule recovery fixture and flyer plate used is shown schematically in Fig. 1. The Fischmeister equation predicts crush strengths for the powders to be ~1.4 GPa. Incorporating experimental densification behavior into AUTODYN [3], a Lagrangian-based hydrocode, an impact velocity of 650 m/s was estimated to achieve near full densification.

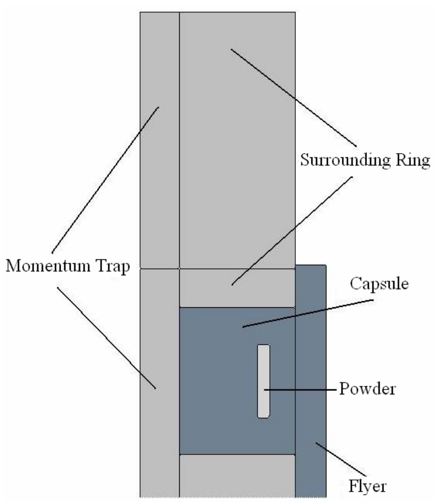

Figure 1. Radial cross-section of one capsule in three capsule experimental setup. Dark gray is 17-4 stainless steel and light gray is Al 6061-T6511.

Impact occurred at 650 m/s, and capsules were recovered from a soft catch tank for retrieval of compacts from within. Compact density was measured through Archimedes' displacement method prior to sectioning. Subsequently, elastic properties of the compacts were determined through ultrasonic measurements. Both longitudinal and shear soundspeeds were measured, yielding direct measurements of Poisson's ratio (ν), Young's modulus (E), and shear modulus (G). Bulk modulus (K) was estimated assuming isotropy of elastic constants. Hardness measurements were taken on the needle cross-section using two series of nano-indentation, each consisting of 10 columns and 12 rows. Micro-indentations covering a similar area were made for all samples; however, the numbers of indentations were reduced to 6-8 per specimen. Fig. 2 shows schematically the arrangement of indentations along the specimen cross-section.

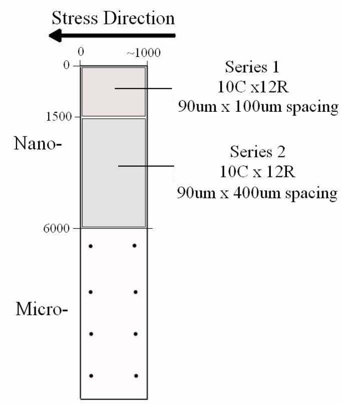

Figure 2. Specimen cross-section indicating placement of indents for nano- (top) and micro- (bottom) hardness.

Electron Backscatter Diffraction (EBSD) orientation maps of the compacted needles cross-section near the impact and rear face were recorded for qualitative comparison with crystallographic orientation and TEM results of starting powders. Also, optical micrographs were taken of the cross-section at the center, middle, and outer radial positions from which montages were stitched together to examine particle deformation and degree of bonding in the axial and radial direction.

RESULTS AND DISCUSSION

Specimens recovered following 650 m/s impact were near fully-dense discs approximately 1 mm thick with average densities ranging from ~96–98% of theoretical. Average density and elastic properties of the compacted samples and bulk Al 6061-T6 are given in Table 2.

Table 2. Density and elastic properties of compacts.

Sample	ρ (g/cm^3)	ν	**E** (GPa)	**G** (GPa)	**K** (GPa)
Equiaxed	2.62	0.27	60.7	23.9	43.8
Needles	2.65	0.29	57.4	22.2	45.8
Platelets	2.59	0.29	53.4	20.6	43.4
Bulk	2.71	0.31	72.4	27.5	63.5

Of the three morphologies, the needles reached the highest density, slightly over 98% of theoretical.

However, the moduli obtained through ultrasonic measurements yield significantly lower values than the bulk material and those reported for a similar density ultrafine-grained (ufg) aluminum with grain sizes between 200-300 nm [4]. This reduction in moduli is attributed to incomplete compaction of particles and porosity near the rear surface of the compact, as observed in optical micrographs of specimen cross-sections.

Nano-indenetation hardness measurements of the needles cross-section yield fairly consistent values for both series of indents, ranging between 1.2 and 1.8 GPa. These values are consistent with those reported for the starting powders [1], suggesting preservation of crystalline structure post-compression. A column averaged hardness map for the needles compact is given in Fig. 3. Micro-indentation resulted in a much larger variation in hardness, ranging between 0.535-1.03 GPa, depending on location of the indent. Micro-hardness values tended to increase approaching the impact face and outer diameter. Similar trends in micro-hardness are observed for all morphology compacts.

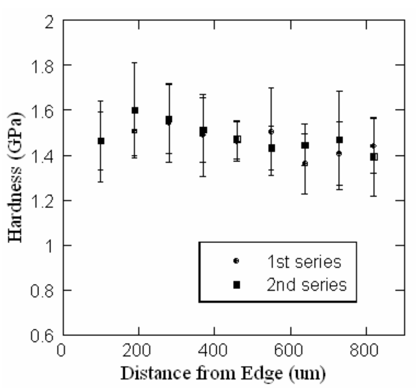

Figure 3. Average column hardness obtained from nano-indentation through thickness of compact.

EBSD data of starting powders shows a strong gradient in grain size from the surface to the particle interior. Near the particle surface grain sizes are on the order of 100-200 nm and tend to increase toward the particle interior, reaching several microns. This trend is also observed in TEM images of the starting powders as shown in Fig. 4.

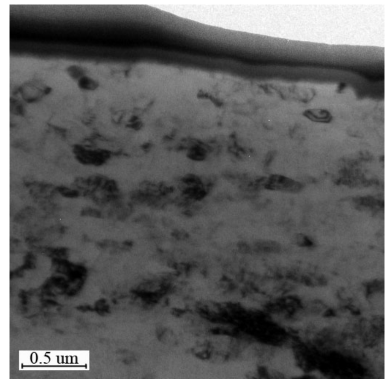

Figure 4. TEM image of equiaxed particle.

EBSD orientation maps of the compacted needles cross-sections differ greatly for sections near the impact and rear surfaces. Near the impact face only a small amount of coherent crystalline regions are observed as shown in Fig. 5.

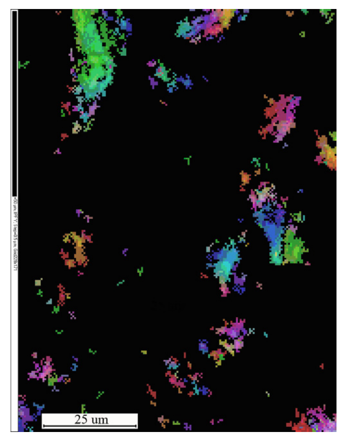

Figure 5. EBSD orientation map of needles cross-section near impact surface. Step size is 0.5um, and impact occurred in horizontal direction.

Several discrete crystallographic regions are present; however, most of the test grid is black indicating either the crystalline regions are too small to detect, or there is a high dislocation density causing incoherency. Toward the rear surface, many more coherent crystalline regions are observed, and EBSD results for a cross-section near the rear surface are shown in Fig. 6. In Fig. 6, it is possible to detect discrete particles, which tend to be elongated in the vertical direction.

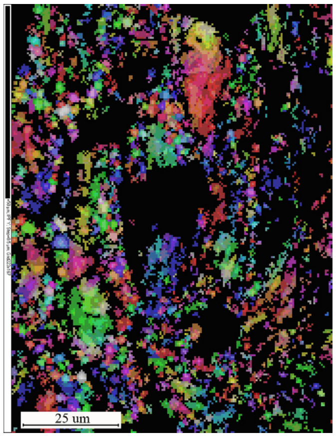

Figure 6. EBSD orientation map of needles cross-section near rear surface. Step size is 0.5um, and impact occurred in horizontal direction.

Boundaries are indicated by thin black regions between the dense observably oriented regions. The observed boundaries could be a result of voids between particles or high dislocation densities on particle surfaces. Exact determination as to their origin can only be obtained through careful coupling of EBSD with optical microscopy and/or TEM. Comparison of EBSD results with optical micrographs taken of the compacted cross-sections suggest the large incoherent regions observed near the impact face are a result of increased plastic deformation. The increased plastic deformation occurring near the impact face can lead to higher dislocation densities and could be responsible for the gradient in coherency observed in the specimen cross-section.

CONCLUSIONS AND FUTURE WORK

Quasi-static compression data has been used to predict dynamic impact conditions necessary to achieve full compaction of aluminum powders to moderate success, with experimental compacts reaching between 96-98% of theoretical density. Moduli values obtained through ultrasonic measurements are low compared to ufg pure aluminum specimens of comparable density. Nano-indentation of compacts exhibit hardness values similar to starting powders, suggesting the microstructure of starting powders is preserved following impact at 650 m/s. EBSD clearly shows this is not the case, especially for particles near the impact face where evidence of coherent crystalline regions is lacking. Further analysis of compact microstructures will be carried out using TEM analysis to determine details of the structure. Micro-indentation shows hardness varying considerably along specimen cross-section, indicative of varying levels of compaction along specimen thickness. This is supported by EBSD and optical microscopy which show a definite gradient in compaction along specimen cross-section, where particles near the impact face exhibit a higher degree of bonding and deformation than those toward the rear. Future work includes determination of elastic-plastic deformation behavior using microsample tensile specimens, and mesoscale simulation of the dynamic compaction event, incorporating real microstructures for all morphologies, to study transient deformation behavior and comparison of final microstructures.

ACKNOWLEDGEMENTS

The authors would like to thank the following people for their technical support: Tom Buchheit, Luke Brewer, Joe Micheal, Steven Younghouse, and Tom Thornhill. Funding for this research is provided by Sandia National Laboratories, a multiprogram laboratory operated by Sandia Corporation, a Lockheed Martin Company, for the United States Department of Energy's National Nuclear Security Administration under Contract DE-AC04-94AL85000.

REFERENCES

1. Shankar, M.R., Chandrasekar, S., Compton, D.W., and King, A.H., "Characteristics of aluminum 6061-T6 deformed to large plastic strains by machining," Material Science and Engineering A, vol. 410, pp. 364-368, 2005.
2. Fishmeister, H. F., and Artz, E., "Densification of powders by particle deformation," Powder Metallurgy, vol. 26, no.2, pp. 82-88, 1983.
3. ANSYS AUTODYN v. 11, Century Dynamics 2006.
4. Legros, M., et al., "Microsample tensile testing of nanocrystalline metals," Philosophical Magazine A, vol. 80, no. 4, pp. 1017-1026, 2000.